

RESEARCH ARTICLE | *Control of Movement*

Done in 100 ms: path-dependent visuomotor transformation in the human upper limb

Chao Gu (顾超),^{1,3} J. Andrew Pruszynski,^{1,2,3,4}  Paul L. Gribble,^{1,2,3} and Brian D. Corneil^{1,2,3,4}

¹Department of Psychology, University of Western Ontario, London, Ontario, Canada; ²Department of Physiology and Pharmacology, University of Western Ontario, London, Ontario, Canada; ³The Brain and Mind Institute, University of Western Ontario, London, Ontario, Canada; and ⁴Robarts Research Institute, University of Western Ontario, London, Ontario, Canada

Submitted 27 November 2017; accepted in final form 2 December 2017

Gu C, Pruszynski JA, Gribble PL, Corneil BD. Done in 100 ms: path-dependent visuomotor transformation in the human upper limb. *J Neurophysiol* 119: 1319–1328, 2018. First published December 6, 2017; doi:10.1152/jn.00839.2017.—A core assumption underlying mental chronometry is that more complex tasks increase cortical processing, prolonging reaction times. In this study we show that increases in task complexity alter the magnitude, rather than the latency, of the output for a circuit that rapidly transforms visual information into motor actions. We quantified visual stimulus-locked responses (SLRs), which are changes in upper limb muscle recruitment that evolve at a fixed latency ~100 ms after novel visual stimulus onset. First, we studied the underlying reference frame of the SLR by dissociating the initial eye and hand position. Despite its quick latency, we found that the SLR was expressed in a hand-centric reference frame, suggesting that the circuit mediating the SLR integrated retinotopic visual information with body configuration. Next, we studied the influence of planned movement trajectory, requiring participants to prepare and generate either curved or straight reaches in the presence of obstacles to attain the same visual stimulus location. We found that SLR magnitude was influenced by the planned movement trajectory to the same visual stimulus. On the basis of these results, we suggest that the circuit mediating the SLR lies in parallel to other well-studied corticospinal pathways. Although the fixed latency of the SLR precludes extensive cortical processing, inputs conveying information relating to task complexity, such as body configuration and planned movement trajectory, can preset nodes within the circuit underlying the SLR to modulate its magnitude.

NEW & NOTEWORTHY We studied stimulus-locked responses (SLRs), which are changes in human upper limb muscle recruitment that evolve at a fixed latency ~100 ms after novel visual stimulus onset. We showed that despite its quick latency, the circuitry mediating the SLR transformed a retinotopic visual signal into a hand-centric motor command that is modulated by the planned movement trajectory. We suggest that the circuit generating the SLR is mediated through a tectoreticulospinal, rather than a corticospinal, pathway.

hand-eye coordination; human reaching movement; movement planning; trajectory; visual response

INTRODUCTION

The reaction time (RT) needed to initiate a visually guided action is a core measure in behavioral neuroscience (Luce 1986). In humans, visually guided reaches from a static posture typically start within ~200–300 ms of stimulus presentation (Welford 1980), with RTs increasing for more complex tasks that require additional cortical processing (Donders 1969). A more precise measurement of RT can be obtained via electromyographic (EMG) recordings of limb muscle activity, which circumvent the electromechanical delays that arise between the neural command to initiate a movement and movement itself (e.g., due to the arm's inertia; Norman and Komi 1979). In addition to the large and well-studied volley of neuromuscular activity that initiates the movement, a brief and small burst of activity occurs time-locked ~100 ms after novel visual stimulus presentation, regardless of the ensuing movement RT (Pruszynski et al. 2010). These visual stimulus-locked responses (SLRs) are directionally tuned, with EMG activity increasing or decreasing for stimulus locations to which the muscle would serve as an agonist or antagonist, respectively. Furthermore, the SLR persists toward the stimulus location even when movement is temporarily withheld (Wood et al. 2015) or proceeds in the opposite direction (Gu et al. 2016).

The SLR evolves during the earliest interval in which visual information can influence limb muscle recruitment, and its short latency limits the opportunity for extensive cortical processing. To better understand the properties of the circuit underlying this rapid sensorimotor transformation, we characterized the SLR across three different visually guided reach experiments by altering task complexity. We studied whether the SLR was expressed in an eye- or hand-centered reference frame by dissociating initial eye and hand position (*experiment 1*) and the influence of different preplanned straight or curved movement trajectories on the SLR (*experiments 2 and 3*). We found that although the SLR latencies remained constant in all three experiments, changes in SLR magnitude showed that the underlying circuit rapidly transforms retinotopic visual information into a hand-centered reference frame in a manner that is influenced by the planned movement trajectory.

Address for reprint requests and other correspondence: B. D. Corneil, Robarts Research Institute, University of Western Ontario, 1151 Richmond St. N, London, ON, Canada N6A 5B7 (e-mail: bcorneil@uwo.ca).

MATERIALS AND METHODS

In total, we had 30 participants (19 men, 11 women; age: 26 ± 5 yr, mean \pm SD) who performed at least one of the three experiments. All were self-declared right-handed except for two left-handed men and two left-handed women. All participants had normal or corrected-to-normal vision and reported no current visual, neurological, and/or musculoskeletal disorders. Participants provided written consent, were paid for their participation, and were free to withdraw from any of the experiments at any time. All procedures were approved by the Health Science Research Ethics Board at the University of Western Ontario. Parts of the apparatus, EMG recording setup, and data analyses have been previously described (Gu et al. 2016; Wood et al. 2015).

Apparatus and kinematics acquisition. Briefly, in all three experiments, participants performed reach movement in the horizontal plane with their right arm while grasping the handle of a robotic manipulandum (InMotion2; InMotion Technologies, Watertown, MA). Participants sat at a desk and interacted with the robotic manipulandum with their elbow supported by a custom-built air sled (see Fig. 1A of Wood et al. 2015). A constant load force of 5 N to the right was applied to increase the baseline activity for the limb muscle of interest for all three experiments. The x - and y -positions of the manipulandum were sampled at 600 Hz. All visual stimuli were presented onto a horizontal mirror, located just below the participant's chin level, which reflected the display of a downward-facing LCD monitor with a refresh rate of 75 Hz. The precise timing of visual stimulus onsets on the LCD screen were determined by a photodiode. The mirror occluded the participant's arm, and visual feedback of the hand was given as a small red cursor.

EMG and electrooculography acquisition. EMG activities from the clavicular head of the right pectoralis major (PEC) muscle were recorded using intramuscular (*experiment 1*) and/or surface recordings (all experiments). Intramuscular EMG activity was recorded using fine-wire electrodes (A-M Systems, Sequim, WA) inserted into the PEC muscle (see Wood et al. 2015 for insertion procedure). Briefly, for each recording we inserted two monopolar electrodes ~ 2.5 cm into the muscle belly of the PEC muscle, enabling recording of multiple motor units. Insertions were aimed ~ 1 cm inferior to the inflection point of the participant's clavicle and were staggered by 1 cm along the muscle's fiber direction. All intramuscular EMG data were recorded with a Myopac Jr. system (Run Technologies, Mission Viejo, CA). Surface EMG was recorded with double-differential electrodes (Delsys, Natick, MA) placed either near or at the same location as the intramuscular recordings. In *experiment 1*, horizontal eye position was measured using bitemporal direct current electrooculography (EOG; Grass Instruments, Astro-Med). EMG and EOG data were digitized and sampled at 4 kHz.

Data analyses. To achieve sample-to-sample matching between kinematic and EMG data, kinematic data were upsampled from 600 to 1,000 Hz with a low-pass interpolation algorithm and then low-pass filtered with a second-order Butterworth filter with a cutoff at 150 Hz. Offline, EMG data were rectified and either integrated into 1-ms bins (intramuscular) or downsampled (surface) to match the 1,000 Hz sample rate. Reach RTs were calculated as the time from the onset of the visual stimulus (measured by a photodiode) to the initiation of the reach movement. Reach initiation was identified by first finding the peak tangential movement velocity and then moving backward to the closest time point at which the velocity profile reached 8% of the peak velocity. We defined the SLR epoch as the period from 85 to 125 ms after stimulus onset. Trials with RTs < 185 ms were excluded to prevent contamination of the SLR epoch by recruitment associated with very short-latency responses (Gu et al. 2016; Wood et al. 2015). We also defined the voluntary movement (MOV) epoch as the period from -20 to 20 ms around the reach RT.

To determine the normalized movement trajectory for *experiments 2* and *3*, we first defined the movement duration for each trial

individually. The movement duration was defined as 50 ms before the time when the hand position surpassed 2 cm from the center of the start position to 50 ms after the time when the hand position surpassed 20 cm (14 cm for the catch trials in *experiment 3*) from the center of the start position. We then interpolated the movement duration into 101 equal time samples. For each normalized time sample, we then extrapolated the x - and y -positions to get the normalized movement trajectory for each trial.

SLR detection and latency analysis. On the basis of previous works identifying the SLR (Corneil et al. 2004; Pruszynski et al. 2010), we used a receiver operating characteristic (ROC) analysis to quantitatively detect the presence of a SLR. In all experiments, we first separated the EMG activity for all correct control reaches based on visual stimulus location and performed the following ROC analysis. For every time sample (1-ms bin) between 100 ms before and 300 ms after visual stimulus onset, we calculated the area under the ROC curve. This metric indicates the probability that an ideal observer could discriminate the side of the stimulus location solely on the basis of EMG activity. A value of 0.5 indicates chance discrimination, whereas a value of 1 or 0 indicates perfectly correct or incorrect discrimination, respectively. We set the thresholds for discrimination at 0.6; these criteria exceed the 95% confidence intervals of data randomly shuffled with a bootstrap procedure (Chapman and Corneil 2011). The earliest discrimination time was defined as the time after stimulus onset at which the ROC was above 0.6 and remained above that threshold for at least 5 of the next 10 samples. On the basis of ROC analyses, we defined the SLR epoch as the period from 85 to 125 ms after visual stimulus onset and categorized any participant with a discrimination time < 125 ms as having a SLR (SLR+ participant). Across the 5 experiments we could reliably detect a SLR in 24 of 30 participants ($\sim 80\%$ detection rates). This rate is comparable to previous reports of the SLR detection on the limb with either intramuscular and surface recordings in this setup (Gu et al. 2016; Wood et al. 2015). To determine the onset latency of the SLR on the upper limb, we used the same procedure as previously described for SLR on neck muscle activity (Goonetilleke et al. 2015). Briefly, we used the same time-series ROC mentioned above and fit a two-piece piecewise linear regression (Cashaback et al. 2013). The first linear regression is based on baseline activity preceding any SLR (from 0 to 80 ms after stimulus onset), and the second linear regression is based on activity for candidate inflection point to the peak of the SLR (maximum ROC value in an interval from 80 to 140 ms). The inflection point was determined as the latency that minimized the sum of the squared error between the observed ROC curve and the two linear regressions. Relative to the ROC value at the inflection point, the onset latency was the time where the ROC increased by 0.05 for the next 5 of 10 samples.

Experiment 1: reference frame task. To initiate each trial, participants ($n = 7/8$; 7 SLR+ participants) brought the cursor into a starting hand position (Fig. 1A, green circle). After a randomized (0.5–1 s) delay, participants had to look toward the starting eye position (red circle). Three different initial positions were possible: either the hand and the eye were in line with the participant's midline (*position 1*), or the hand was 10 cm to the right and the eye was 10 cm to left of midline (*position 2*), or vice versa where the hand was 10 cm to the left and the eye was 10 cm to the right of midline (*position 3*). After another randomized (1–1.5 s) delay, a black visual stimulus appeared concurrently with the offset of both the starting hand and eye position stimuli. This served as the go cue to make a coordinated hand-eye movement toward the black visual stimulus. The black stimulus could be in one of three possible locations: either at the midline (Stim_C) or 20 cm to the left (Stim_L) or right of midline (Stim_R). Participants had to reach to the stimulus location to start the next trial. In the case of *position 1* and Stim_C, the participant did not have to move; the next trial started 1 s after stimulus onset. If the participant moved their hand outside of the starting hand position at any point before the onset of the black stimulus, the trial was aborted and reset. Each participant

performed 8 blocks, with each block consisting of 72 trials, in which the 9 different trial types (3 start positions \times 3 stimulus locations) were tested pseudorandomly 8 different times per block. For Stim_C in *position 1*, participants were not required to move. To analyze the data during the presumed MOV epoch on these trials, we assumed that the RT for these trials would be from a similar distribution of RT as Stim_L and Stim_R reach movements. Thus we randomly assigned a reach RT for each Stim_C trial from the pooled RT of Stim_L and Stim_R in *position 1*.

Experiment 2: obstacle task. Each trial began with the appearance of a start position stimulus; on two-thirds of all trials, the gray visual obstacle was presented concurrently. No obstacle was presented on the other one-third of trials, which served as a control condition. Two different sets of obstacles could appear, either a horizontal bar or two upside-down L-shaped obstacles (Fig. 2). To initiate the trial, participants ($n = 15/20$ SLR+) moved the cursor into the start position. After a variable delay (1–1.25 s), a black peripheral stimulus appeared 20 cm from the position, at either a left-outward [135° counterclockwise (CCW) from straight right] or right-outward (45° CCW) location away from the participant. The start position was extinguished simultaneously with the presentation of the peripheral stimulus. Participants then had to move the cursor as quickly as possible to the peripheral stimulus. Each participant performed four blocks; in two blocks participants were instructed to avoid the gray obstacles, whereas in the other two blocks they were instructed to reach through the obstacles when reaching for the peripheral stimulus. The order of instruction was counterbalanced across participants. Each block consisted of 150 trials in total, with 25 trials for each of the 6 different conditions.

Experiment 3: choice task. Each trial began with the appearance of a start position stimulus and a gray obstacle (Fig. 3A). To initiate the trial, participants ($n = 14/15$ SLR+) moved the cursor into the start position. After a variable delay (1–1.25 s), the start position was extinguished simultaneously with the presentation of the peripheral black visual stimulus. On test trials (2/3 of all trials), the peripheral stimulus was presented 20 cm left-outward from the start position (135° CCW), whereas in catch trials (1/3 of all trials), the peripheral stimulus was presented 14 cm from the start position directly outward (90° CCW) or leftward (180° CCW) with equal likelihood. Participants were instructed to move the cursor as quickly as possible to the peripheral stimulus while avoiding the gray obstacle by choosing the shortest movement trajectory. The shape of the gray obstacle varied on a trial-by-trial basis, but the overall area remained constant. The obstacle shape displayed was based on an adaptive estimation of the psychometric function for each participant. We assumed that the psychometric function of the choice of the movement trajectory around the obstacle took the form of a logistic function (Eq. 1):

$$p(x) = \frac{1}{1 + e^{\beta(x-\alpha)}} \quad (1)$$

in which x is the shape of the obstacle (ranging from a purely horizontal bar, $x = -68$, through L-shaped obstacles, to a vertical bar, $x = 68$; for shapes, see x -axis of Fig. 3B), $p(x)$ indicates the probability of leftward curved reach around the obstacle for the given obstacle shape; and α and β are the threshold and slope of the logistic function, respectively. To estimate this function, we used a modified updated maximum likelihood procedure (Shen and Richards 2012), with the parameter space consisting of a grid of α and β values. The α parameter spanned 69 values ranging from -68 to 68 in 2-unit increments. The β parameter spanned values ranging from 0 to 0.5 in increments of 0.05. A uniform prior ($\alpha, \beta = 0$) was used for the 1st block, whereas subsequent blocks used the estimated parameters from the last trial of the previous block. To initialize each block, the first 5 trials had obstacles that were at the 0th, 100th, 50th, 25th, and 75th percentiles ($x = -68, 68, 0, -34, 34$ units, respectively). Afterward, the obstacle shape was set either at the estimated threshold, $p(x) = 0.5$, or at either the lower, $p(x) = 0.25$, or upper deflection,

$p(x) = 0.75$, in a pseudorandom order at a 2:1:1 ratio. Test, catch leftward, and catch rightward trials were also presented in a pseudorandom order at a 4:1:1 ratio, respectively. Each participant performed 6 blocks, except for one who performed 5 blocks, with each block consisting of 197 trials: 5 initial trials, 128 test trials, 32 catch leftward trials, and 32 catch outward trials. All participants had at least 100 correct test trials for the threshold visual obstacle, for which $p(\text{leftward})$ was closest to 0.5.

Experimental design and statistical analysis. All statistical analyses were performed with custom-written script in MATLAB (version R2014b; The MathWorks, Natick, MA). In *experiment 1*, the within-subjects analysis was a two-way ANOVA with the mean factors of start position and stimulus location, whereas the between-subjects analysis was a one-way ANOVA for the mean adjusted normalized EMG activity of each start position. In *experiment 2*, the within-subjects analysis was a two-way ANOVA with the mean factors of stimulus location and movement trajectory, whereas the between-subjects analysis was a one-way ANOVA of the normalized EMG activity for movement trajectory. Finally, in *experiment 3*, for both within- and between-subjects analyses, we performed a two-way ANOVA with the mean factors of initial reach direction (i.e., leftward or outward) and movement trajectory (i.e., straight or curved). The level of significance was set to $P < 0.05$ at the group level and $P < 0.05$ using Tukey's honestly significant difference (HSD) correction for post hoc comparisons.

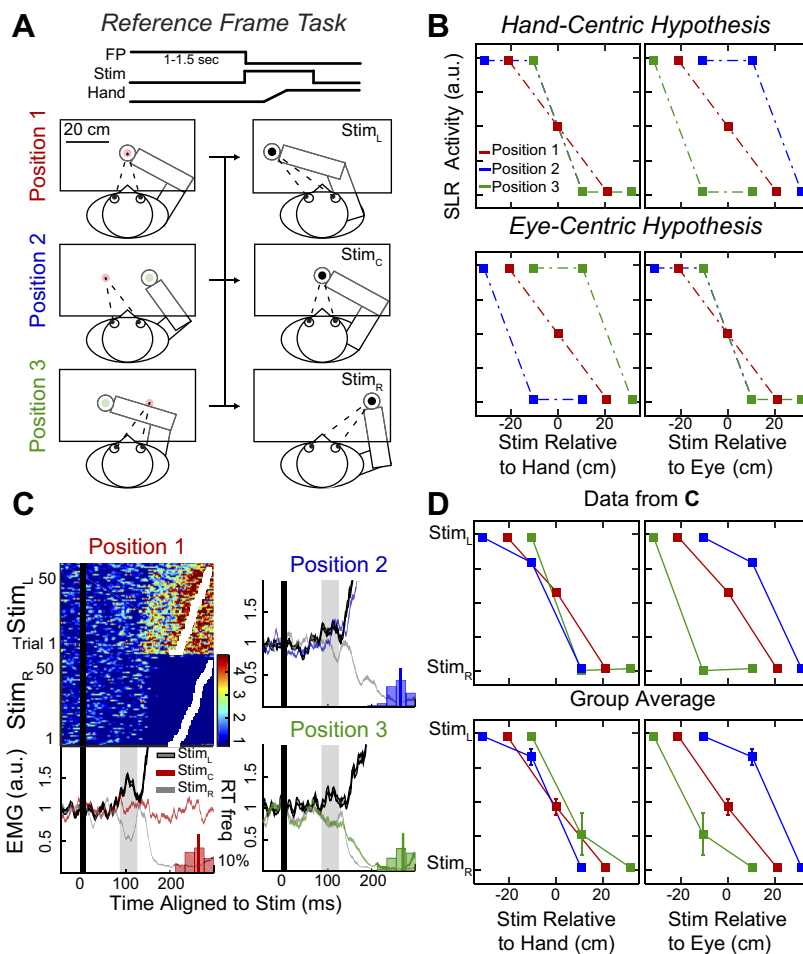
RESULTS

In total, 30 participants took part in at least one of the three experiments (42 separate sessions in total). Across all three experiments, a reliable SLR was detected in 24 of 30 participants (SLR+, 80%; see MATERIALS AND METHODS for detection criteria). This SLR detection rate was similar to that in our previous studies (Gu et al. 2016; Wood et al. 2015). Data from participants who did not exhibit a SLR were excluded from all subsequent analyses.

The SLR encodes stimulus location relative to hand, not eye, position. Although previous studies have reported that SLRs are tuned to the position of the visual stimulus (Gu et al. 2016; Pruszynski et al. 2010; Wood et al. 2015), these studies did not manipulate the initial position of the eyes and hand and thus could not differentiate whether the SLR encoded stimulus position relative to the eye or hand. The underlying reference frame of the SLR may start to reveal the underlying neural circuitry, since many functional MRI and neurophysiological studies have shown that visual stimuli can be encoded in different reference frames throughout the parietal and motor cortices (Batista et al. 1999; Buneo et al. 2002; Crawford et al. 2004; Medendorp et al. 2003; Pesaran et al. 2006).

In *experiment 1*, we assessed whether the SLR encoded stimulus location relative to the eye (an eye-centric reference frame) or the hand position (a hand-centric reference frame). Participants ($n = 7/8$; 7 SLR+ participants) began each trial in one of three initial positions (Fig. 1A), with the hand and eye in line with the participant's midline (*position 1*; red), with the hand 10 cm right and the eye 10 cm left of midline (*position 2*; blue), or with the hand 10 cm left and the eye 10 cm right of midline (*position 3*; green). Participants then made a coordinated hand-eye movement toward a black visual stimulus that appeared either 20 cm left (Stim_L), 20 cm right (Stim_R), or at the midline (Stim_C). These various initial positions and stimulus locations allowed us to predict SLR magnitude as a function of stimulus location relative to either the hand or eye position (Fig. 1B). Note that if the SLR magnitude is plotted as

Fig. 1. The SLR generates a motor command toward the visual stimulus in a hand-centric reference frame. **A**: experimental paradigm. Participants started in 1 of 3 different initial positions, and after at least 1 s moved both their eyes and right hand to a black visual stimulus. **B**: these various initial positions and stimulus locations allowed us to predict SLR magnitude as a function of stimulus location relative to either the hand (hand-centric reference frame; *top*) or the eye (eye-centric reference frame; *bottom*). a.u., Arbitrary units. **C**: individual and mean EMG activity from a participant. The color maps show individual Stim_L and Stim_R trials from *position 1*. Each row represents EMG activity from a single trial, with all trials aligned to stimulus onset (black line) and sorted on the basis of reach RT (white squares). Data in all other subpanels represent mean \pm SE EMG activity for correct trials, segregated by initial position and stimulus location. Overlaid on each mean EMG plot are the RT distribution (bars) and median RT (vertical line) for each position. Gray-shaded boxes indicate the SLR epoch. **D**: the individual (participant in **C**; *top*) and the group ($n = 7$, *bottom*) mean adjusted normalized SLR magnitudes conform to the prediction of a hand-centric reference frame.



a function of stimulus eccentricity in the correct reference frame, then such functions should overlap for the three different starting positions. In contrast, such functions should be staggered if plotted in the incorrect reference frame (Fig. 1B).

Figure 1C shows a participant's EMG activity aligned to visual stimulus onset (black line) from all three initial positions. Trials were segregated on the basis of initial position and visual stimulus location. EMG activity was normalized to baseline activity (mean EMG activity 41 ms before stimulus onset) for each position separately. In *position 1*, similar to previous reports, we observed a reliable difference in SLR magnitude (shaded box spanning 85–125 ms after stimulus onset; Fig. 1C, *bottom left*) between Stim_L and Stim_R trials [2-way ANOVA, start position and stimulus location, interaction effect: $F_{(4,553)} = 4.88$, $P = 0.0007$; post hoc Tukey's HSD, $P < 10^{-7}$]. This increase and decrease in EMG activity also could be seen on individual EMG traces from the Stim_L and Stim_R trials, respectively (Fig. 1C, *top left* and *middle left*). The SLR was relatively brief and evolved before the much larger change in EMG activity associated with either the leftward or rightward reach movement (RTs denoted by white squares). The SLR persisted in the other two initial positions, with SLR magnitude being reliably greater for Stim_L compared with Stim_R trials (Fig. 1C, $P = 0.0002$ and $P < 10^{-6}$ for *positions 2* and *3*, respectively). Across all participants, we found no difference in the onset latency of the SLR for Stim_L and Stim_R trials between when the hand and eye started in the

same (*position 1*; latency = 87.4 ± 1.2 ms, mean \pm SE) vs. different locations (*positions 2* and *3*; 86.7 ± 2.2 ms; paired t -test: $t_6 = 0.28$, $P = 0.79$), even though the median RTs were slightly shorter when the eye and hand started at the same (272.4 ± 9.4 ms) vs. different positions (286.0 ± 11.2 ms; paired t -test: $t_6 = -3.1$, $P = 0.02$).

In *positions 2* and *3*, the Stim_C trials (color trials) can be used to differentiate between hand-centric and eye-centric reference frames, because the stimulus falls between the initial positions of the hand and eye. In *position 2*, SLR magnitude increased relative to the baseline activity by an equal amount for both Stim_C and Stim_L trials ($P = 0.89$) when the stimulus fell to the left of the hand. In *position 3*, SLR magnitude decreased by an equal amount for both the Stim_C and Stim_R trials ($P = 0.99$) when the stimulus fell to the right of the hand. Thus, for this participant, the pattern of SLR magnitudes was consistent with a hand-centric reference frame. To account for the differences in SLR magnitude for each position and across all participants, we scaled the SLR magnitude for Stim_C trials on the basis of the SLR magnitudes observed for Stim_L and Stim_R trials (+1, -1 arbitrary unit, respectively). This allowed us to test our data against the two initial predictions, expressing the adjusted normalized SLR magnitudes aligned to stimulus location relative to either the hand or eye position for this participant (Fig. 1D, *top row*) and across the group (*bottom row*). Our results clearly indicate that the SLR is encoded in a hand-centric reference frame (compare with the hand-centric

hypothesis in Fig. 1B). Across the group, we found reliably greater SLR magnitudes for Stim_C trials in *position 2* compared with *position 3* [1-way ANOVA, start position: $F_{(2,18)} = 7.64$, $P = 0.004$; post hoc Tukey's HSD, $P = 0.003$]. We found a similar response pattern during the MOV epoch, where *position 2* evoked a greater MOV response compared with *position 3* [$F_{(2,18)} = 302.8$, $P < 10^{-13}$; post hoc Tukey's HSD, $P < 10^{-8}$]. This result suggests that despite its short latency, the circuit mediating the SLR rapidly integrates visual stimulus location and the underlying body position, generating a motor command in a hand-centric reference frame.

Movement trajectory influences SLR magnitude for reaches to the same visual stimulus. Given that the SLR encoded the visual stimulus relative to the current hand position, we next examined if the SLR simply encodes visual stimulus location in space or if it is influenced by the planned movement trajectory. To start differentiating these two possibilities, in *experiment 2*, participants ($n = 15/20$ SLR+) performed either curved or straight reaches to two potential visual stimulus locations. In different blocks, participants were instructed to either avoid or reach through different visual obstacles to attain the left-outward or right-outward visual stimulus. Except for control trials without the obstacle, obstacles were present at trial onset so that participants could plan their trajectory to the two potential stimulus locations. Figure 2 shows the mean normalized movement trajectories and EMG activities when a participant avoided (Fig. 2A) or reached through (Fig. 2B) the obstacle. Trials were categorized on the basis of movement trajectories: straight, with no obstacle (control; black); straight, either avoiding or reaching through an obstacle (straight; red); or curved, either avoiding or reaching through an obstacle (curved; blue). When categorized this way, we found no reliable difference in mean SLR magnitude across our sample for avoiding compared with reaching through the different visual obstacles [3-way ANOVA, stimulus location, movement trajectory, and instruction, main effect for instruction: $F_{(1,175)} = 0.03$, $P = 0.85$]. Thus all subsequent analyses examined mean SLR magnitudes as a function of stimulus location and movement trajectory.

Figure 2C, *top*, shows the same participant's EMG data, but with the EMG activity combined between the two different instructions. To compare the difference in SLR magnitude (Δ SLR magnitude) between curved and straight reach trials, we calculated the mean EMG difference between left-outward and right-outward stimulus locations (Fig. 2C, *bottom*) during the SLR epoch for the three different movement trajectories. Once again, across all participants, we could not find a difference in SLR latency between straight and curved trajectories (95.1 ± 1.6 and 99.8 ± 2.8 ms, respectively; paired t -test: $t_{14} = -1.9$, $P = 0.07$). Note the increase in SLR latency compared with that in *experiment 1* is probably due to the change in stimulus locations, because left- and right-outward are not the preferred and nonpreferred directions of the SLR (Pruszynski et al. 2010). Instead, we did find a reliable decrease in Δ SLR magnitude for Curved reaches compared with both control and straight reaches [Fig. 2D; 1-way ANOVA, movement trajectory: $F_{(2,42)} = 17.53$, $P < 10^{-5}$; post hoc Tukey's HSD, $P = 0.001$ and $P < 10^{-4}$, respectively]. The decrease in Δ SLR magnitude between curved and straight reaches was likely not due to a potential confound of increased RTs (Gu et al. 2016; Pruszynski et al. 2010), because curved

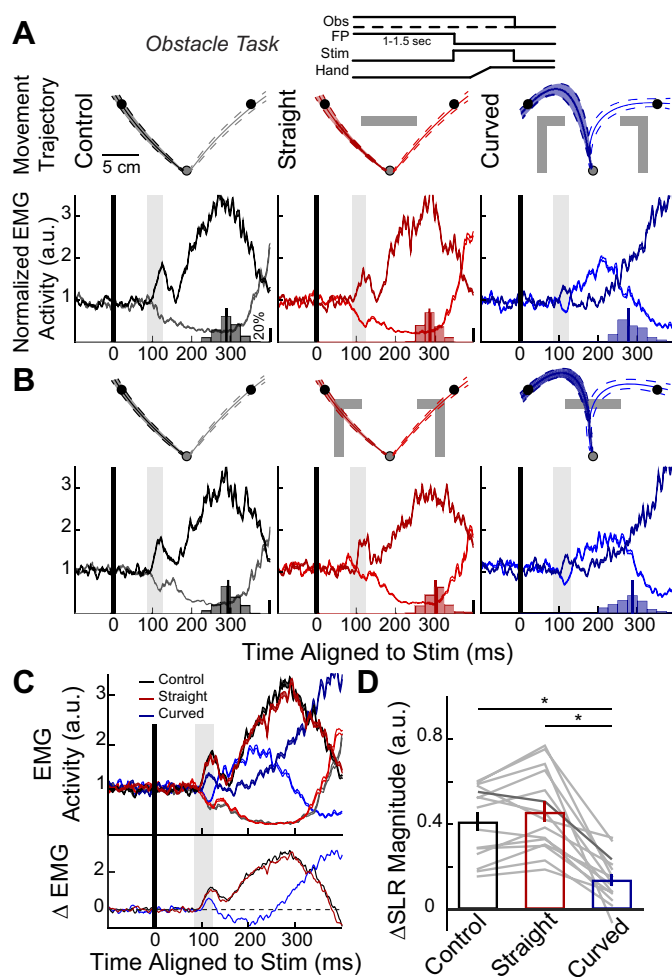


Fig. 2. Decreased SLR magnitude for curved compared with straight reaches to the same visual stimulus. *A* and *B*: kinematic and EMG data from a participant during the obstacle task when instructed to avoid or reach through the visual obstacle (gray rectangles). Left-outward (dark-shaded contours) and right-outward (light-shaded contours) reach trials were segregated by movement trajectory: reaches with no obstacles (control; black), straight reaches with obstacles (straight; red), or curved reaches with obstacles (curved; blue). All obstacles were shown to the participants for at least 1 s before the onset of the peripheral visual stimulus. *Top* panels show the mean (\pm SD) normalized movement trajectories for each condition, whereas *bottom* panels show the corresponding mean (\pm SE) EMG activities aligned to stimulus onset, with the SLR epoch highlighted (gray-shaded boxes). Overlaid on each mean EMG plot are the RT distribution (bars) and median RT (vertical line) for condition. *C*, *top*: the same EMG data as *A* and *B*, but with EMG data combined for the 3 difference movement trajectories regardless of visual obstacle and task instruction. *Bottom*: the difference in mean EMG activity (Δ EMG) between left-outward and right-outward reach trials for the 3 trajectories. *D*: group mean (\pm SE) Δ EMG during the SLR epoch (Δ SLR magnitude) for the 3 different movement trajectories. Each gray line represents an individual participant, with the darker gray line representing data from the participant in *C*. * $P < 0.0001$.

reaches had shorter median RTs than straight reaches (268.1 ± 6.6 and 277.3 ± 6.4 ms, respectively; paired t -test: $t_{14} = 2.76$, $P = 0.015$). Next, we reexamined the EMG activity during the MOV epoch. As expected given the initial outward trajectory for the curved reaches, which is associated with less PEC muscle recruitment, EMG activity for the MOV response was also attenuated for curved compared with control and straight reaches [$F_{(2,42)} = 10.1$, $P = 0.0003$; post hoc Tukey's HSD, both $P = 0.001$]. However, it was not the case that EMG

activity during the SLR simply correlated with a given initial movement trajectory, because the SLR still differed between left-outward vs. right-outward stimulus locations for curved reaches (Fig. 2). These results suggest that the SLR is not simply encoding either the spatial location of a stimulus or the movement trajectory, but rather that the SLR to a given stimulus location is modulated by the planned movement trajectory.

Initial movement trajectory, not task demand, influences SLR magnitude for curved reaches. A potential confound in *experiment 2* was the overall difference in task demand related to planning a curved vs. a straight reach movement. Previous work has shown that curved reaches were more task demanding than straight point-to-point reaches (Wong et al. 2016), and we previously showed that SLR magnitude decreased with increase task demands, i.e., when participants had to move away rather than toward a visual stimulus (Gu et al. 2016). In *experiment 3*, we controlled for task demand by having participants ($n = 14/15$ SLR+) perform two different curved reach trajectories to attain the same visual stimulus (Fig. 3A). At the beginning of each trial, a visual obstacle, which participants were instructed to avoid, was shown. In test trials, participants made either an initially leftward (dark red) or outward (light red) curved movement to a left-outward stimulus. We varied the shape of the obstacle on a trial-by-trial basis (see MATERIALS AND METHODS, *Experiment 3: choice task*, for exact detail). Figure 3B shows the probability of a leftward curved reach as a function of the possible obstacle shape. The obstacle where $p(\text{leftward}) \approx 0.5$ was preferentially sampled and termed the threshold obstacle (filled circle). In addition, we interleaved catch trials so that participants made straight leftward (black) and outward (gray) movements that had initial trajectories similar to those of the curved movements (see insets for movement trajectories in Fig. 3, C and E). Once again, we found no difference in the SLR latency for curved vs. catch trials (95.9 ± 1.3 and 101.3 ± 4.1 ms, respectively; paired t -test: $t_{13} = 1.33$, $P = 0.21$).

To analyze this data set, we first pooled all correct trials together regardless of the obstacle's shape for a single participant. On catch trials, the SLR magnitude was greater for leftward compared with outward straight reaches [Fig. 3C; 2-way ANOVA, initial direction and trajectory type, interaction effect: $F_{(1,1113)} = 5.31$, $P = 0.02$; post hoc Tukey's HSD, $P < 10^{-8}$]. Similarly, on test trials, the SLR magnitude was also greater for leftward compared with outward curved reaches ($P < 10^{-8}$). When we compared reaches with the same initial movement trajectory (straight vs. curved reaches), we found no reliable difference in SLR magnitudes for both initially leftward and outward reaches ($P = 0.15$ and $P = 0.68$, respectively). To further examine the influence of the planned movement trajectories on the SLR magnitude, we next examined trials at the threshold obstacle, where the exact same visual obstacle was presented and the participant generated leftward or outward curved movement trajectories approximately half the time [$p(\text{leftward}) = 0.55$; filled circle in Fig. 3B]. As before, the SLR magnitude was greater for leftward vs. outward reaches for both catch and test trials [Fig. 3E; 2-way ANOVA, interaction effect: $F_{(1,279)} = 41.4$, $P < 10^{-9}$; post hoc Tukey's HSD, $P < 10^{-8}$ and $P = 0.03$, respectively]. Furthermore, the SLR magnitudes were not different for straight vs. curved reaches with the same initial trajectory ($P =$

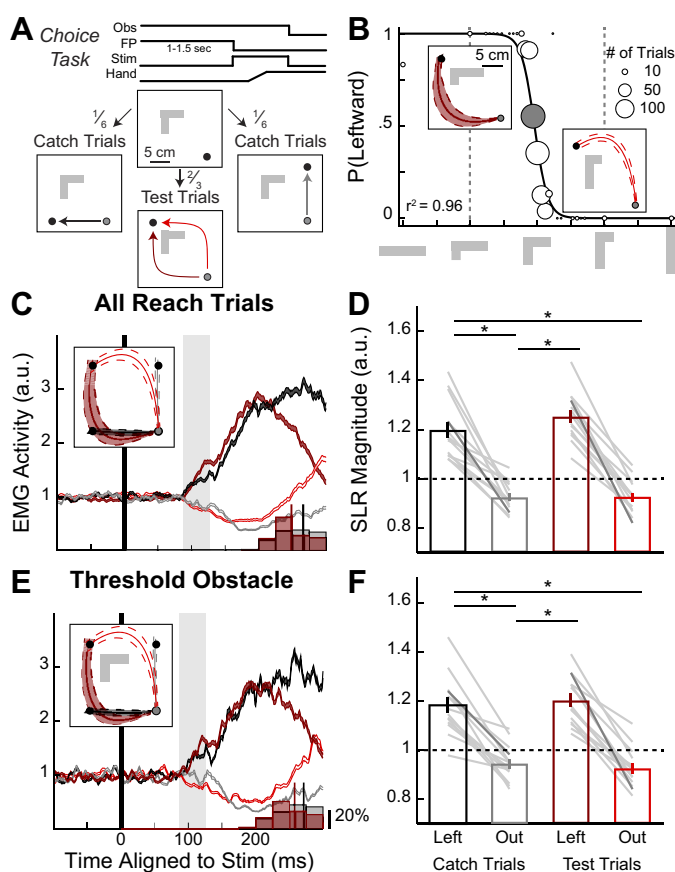


Fig. 3. SLR magnitude modulated by preplanned movement trajectory. **A:** experiment paradigm. Participants were instructed to reach to a visual stimulus by using the shortest movement trajectory while avoiding an obstacle. The shape of the obstacle varied on a trial-by-trial basis (see MATERIALS AND METHODS for exact details). For test trials, participants made either initially curved leftward (dark red arrow) or outward (light red arrow) reaches toward a left-outward visual stimulus. For catch trials, participants reached straight leftward (black arrow) or outward (gray arrow). Once again, the obstacle was presented at least 1 s before the onset of peripheral visual stimulus. **B:** behavioral performance for all test trials from a participant. The probability of an initial leftward curved reach is plotted as a function of obstacle shape. *Insets* show the mean (\pm SD) normalized movement trajectories for 2 different obstacle shapes. Black line is the best fit of a logistic function (Eq. 1) to the participant's behavior. **C** and **E:** the participant's mean (\pm SE) EMG for the different reach types for all reach trials (**C**) and for the threshold obstacle (**E**; shaded circle from **B**) aligned to stimulus onset. Overlaid on each mean EMG plot are the RT distribution (bars) and median RT (vertical line) for curved and straight reaches. **D** and **F:** group mean (\pm SE) SLR magnitudes for all reach trials (**D**) and for the threshold obstacle (**F**) for the 4 different reach conditions. Each gray line represents an individual participant, with the darker gray line indicating data from the participant in **B**. * $P < 10^{-6}$.

0.31 and $P = 0.78$, for initially leftward and outward reaches, respectively).

We observed the same pattern of SLR magnitude modulation based on initial movement trajectory across all participants: SLR magnitude was greater for leftward vs. outward reaches when pooled for all obstacles (Fig. 3D) and for the threshold obstacle (Fig. 3F; 2-way ANOVA, main effect of direction: $F_{(1,52)} = 160.44$ and 104.64 , both $P < 10^{-13}$; post hoc Tukey's HSD, all $P < 10^{-9}$). Again, we found no differences in SLR magnitude for the same initial movement trajectory (all $P > 0.38$). Thus, even when we controlled for task demand by having participants perform curved reaches with different initial trajectories to the same visual stimulus loca-

tion, we found that the SLR was still modulated by the initial movement trajectory. Likewise, when we reexamined the data for the MOV response, we found increased PEC muscle recruitment for leftward vs. outward movement trajectories [2-way ANOVA, main effect of direction: $F_{(1,52)} = 129.38$ and 138.43 , both $P < 10^{-14}$; post hoc Tukey's HSD, all $P < 10^{-9}$]. Thus SLR magnitude for the same visual stimulus is modulated by the initial planned movement trajectory.

SLR magnitude during catch trials was modulated on the basis of preplanned movement. Finally, to further demonstrate that the SLR magnitude was modulated on the basis of preplanned movement, we further examined the SLR on catch trials. Recall that catch trials were randomly interleaved throughout the experiment, appearing at the leftward or outward locations regardless of obstacle shape. Given that the obstacle was present at the start of the trial, catch trials could be classified as being either congruent (i.e., the preplanned movement was in the same direction as the catch trial) or incongruent (i.e., the preplanned movement was in the opposite direction; Fig. 4A). For example, obstacles more horizontal than the threshold obstacle (light gray shaded region in Fig. 4A) were congruent for leftward and incongruent for outward catch trials. In contrast, obstacles more vertical than the threshold obstacle (nonshaded region in Fig. 4A) were congruent to outward and incongruent to leftward catch trials.

Figure 4B shows the mean EMG activity for all catch trials when we separated for both direction (leftward, black; outward, gray) and congruency (congruent, filled; incongruent, open). Note that we observed a reliable difference in EMG activity during the SLR epoch for both congruent and incongruent trials, but the magnitude of the SLR was smaller for incongruent trials. Figure 4C shows the mean Δ SLR magnitude (leftward – outward catch trials; black) and median RT (gray) across all participants for congruent and incongruent trials. We found a reliably larger Δ SLR magnitude for congruent compared with incongruent trials (paired t -test: $t_{13} = 6.88$, $P < 10^{-4}$), but the incongruent Δ SLR magnitude was still present (1-sample t -test: $t_{13} = 2.71$, $P = 0.018$). Consistent with the changes in Δ SLR magnitude, we also observed a difference in the ensuing RT, where participants had substantially shorter RTs for congruent compared with incongruent trials

(262.8 ± 5.7 and 288.9 ± 6.9 ms, respectively; paired t -test: $t_{13} = -6.55$, $P < 10^{-4}$).

DISCUSSION

In the present study, we characterized the visual stimulus-locked response (SLR) on the human pectoralis major muscle during three different visually guided reach tasks. Previous work has shown that the SLR is the first wave of muscle recruitment that is evoked by the onset of a novel visual stimulus, occurring within 100 ms of stimulus onset and preceding the larger volley of EMG activity associated with movement initiation (Pruszynski et al. 2010; Wood et al. 2015). The design of each task was based on earlier work conducted in either human or nonhuman primates, allowing for a direct comparison of SLR measurements to neurophysiological and behavioral concepts of sensorimotor control of reaching. The outcomes of these three experiments can be summarized into three main points. First, the onset latency of the SLR does not change with increases in task complexity during any of the three experiments. Second, the SLR is directionally tuned to the stimulus location relative to the hand, not eye, position. Finally, the SLR magnitude is influenced by, but not completely determined by, the preplanned initial movement trajectory.

There are many similarities between the SLR's visuomotor properties, which are evoked from a static posture, and rapid online corrective reaching movements to displaced visual (Gaveau et al. 2014) or tactile stimuli (Pruszynski et al. 2016). For example, the ~100-ms latency of the SLR is consistent with previous reports of EMG response latencies to a displaced visual stimulus (Fautrelle et al. 2010; Soechting and Lacquaniti 1983) and occurs early enough to change reach kinematics within ~150 ms (Carlton 1981). Like the SLR, the latency of the online corrective movement is not modulated by changes in task demand (Franklin et al. 2016; Oostwoud Wijdenes et al. 2011). In an anti-reach paradigm, both the SLR (Gu et al. 2016) and the initial trajectory of the corrective movements (Day and Lyon 2000) are invariably directed toward the stimulus, even though the participants eventually moved in the opposite direction. Additionally, both the SLR (Fig. 1) and corrective movements (Diedrichsen et al. 2004) are encoded in a hand-centric reference frame, reflecting stimulus location relative to the hand regardless of current eye position. Given

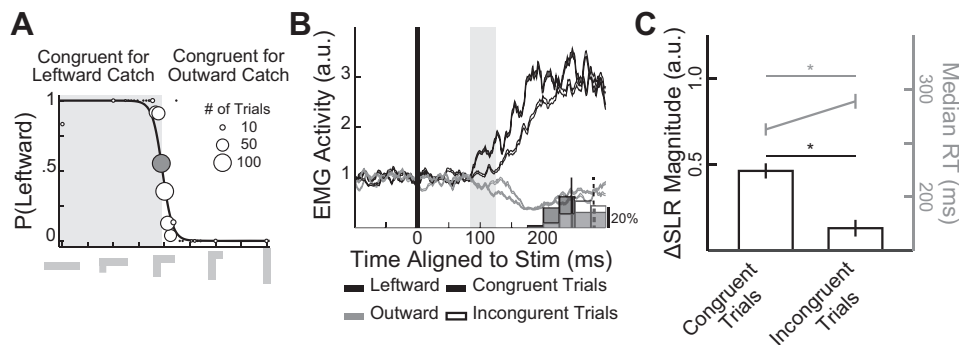


Fig. 4. SLR magnitude and RT modulation for catch trials based on obstacle shape. A: catch trials were separated into congruent and incongruent trials. Leftward congruent and incongruent trials were any trials with an obstacle more horizontal (gray-shaded region) and vertical (nonshaded region) than the threshold obstacle (filled circle), respectively. Outward trials were the opposite, where congruent and incongruent trials were more vertical and horizontal than the threshold obstacle, respectively. B: mean (\pm SE) EMG activity for congruent (filled) and incongruent (open) catch trials sorted by either leftward (black) or outward (gray) stimulus location from the same participant as in Fig. 3. Overlaid on each mean EMG plot are the RT distributions (bars) and median RT (vertical lines) for curved and straight reaches. C: mean (\pm SE) Δ SLR magnitude (leftward – outward; black) and median RT (gray) for both congruent and incongruent trials across all participants. * $P < 10^{-4}$.

the similarities between the SLR and corrective reach movements, we suggest that both are driven by a fast visuomotor system that lies in parallel to the well-studied corticospinal pathways (Alstermark and Isa 2012).

It is tempting to speculate about the pathway that could be underlying the SLR and, by extension, corrective reach movements. Our findings are consistent with previous suggestions that corrective movements are mediated by visual inputs relayed through the superior colliculus (SC) via the reticulospinal pathway (Day and Brown 2001; Reynolds and Day 2012). For example, many neurons in intermediate and deep layers of the SC discharge a volley of action potentials within 50 ms of visual stimulus onset (Wurtz and Goldberg 1972) that depends on the integrity of the lateral geniculate nucleus and primary visual cortex (Schiller et al. 1979). Moreover, axons of these visually responsive SC neurons contribute to the descending predorsal bundle that branches into the reticular formation (Rodgers et al. 2006), leading to SLRs on neck muscles that promote orienting head movements (Corneil et al. 2004, 2008; Rezvani and Corneil 2008). In addition to its role in oculomotor control, the SC also plays a more general role in whole body orienting (Corneil and Munoz 2014; Gandhi and Katnani 2011) and proximal limb control (Lünenburger et al. 2001). Stimulation (Philipp and Hoffmann 2014) and chemical inactivation (Song et al. 2011) of the SC can influence reaching behavior in nonhuman primates, in line with human imaging studies of selective SC blood oxygen level-dependent (BOLD) activation during reaching tasks (Himmelbach et al. 2013; Linzenbold and Himmelbach 2012). Reach-related SC neurons can also exhibit similar short-latency visual responses (Song and McPeck 2015), and movement-related activity correlates with recruitment of proximal limb muscle activity (Stuphorn et al. 1999; Werner et al. 1997). Furthermore, like the SLR, a subset of these neurons operate in a hand-centric reference frame (Stuphorn et al. 2000).

Others have proposed that corrective movements are mediated through a cortical pathway, specifically via the posterior parietal cortex (PPC; Desmurget et al. 1999; Pisella et al. 2000). The ~100-ms latency of the SLR and its expression in hand-centric reference frame are both inconsistent with the known properties of PPC activity. For example, the SLR latency in the human limb occurs at or around the same time as the peak of the visual response of the monkey PPC (Snyder et al. 1998). Most of these visual responses also are not encoded in a hand-centric reference frame that we observed with the SLR (Batista et al. 1999; Buneo et al. 2002). Thus, although the PPC may be involved in the later phases of online corrections (Franklin et al. 2016), it seems unlikely that the PPC is involved in generating the SLR. Additionally, although primary motor cortex and premotor cortex do exhibit rapid visual transient responses (Kwan et al. 1981; Weinrich and Wise 1982), a recent study has suggested that these visual transient responses do not affect the neural output in both primary and premotor cortices (Stavisky et al. 2017).

Finally, the results shown in *experiments 2* and *3* demonstrate that advanced planning of a movement trajectory can influence SLR magnitude. In both experiments, participants viewed an obstacle they either had to avoid or intersect with for an extended period of time before the presentation of the visual stimulus. Moreover, the stimuli could only appear at a limited number of locations (2 and 3 for *experiments 2* and *3*, respectively). The

influence of such advanced planning on the SLR is particularly apparent in catch trials in *experiment 3*, where congruent stimulus location in line with the initial phase of the planned curved trajectory evoked a larger SLR than incongruent stimulus location (Fig. 4). Importantly, such advanced planning did not influence baseline EMG activity just before the SLR epoch. Previous neurophysiological studies have shown anticipatory build-up neural activity well before movement onset to both spatial and nonspatial cues throughout the primary (Confais et al. 2012; Tanji and Evarts 1976) and premotor cortices (Cisek and Kalaska 2005; Mauritz and Wise 1986), as well as within the PPC (MacKay and Crammond 1987; Snyder et al. 2006); however such anticipatory activity did not lead to EMG recruitment. Furthermore, other studies also have shown that advanced planning of multiple alternatives did not lead to increased EMG activity or behavioral output during the planning phase (Cisek and Kalaska 2005; Klaes et al. 2011; Stewart et al. 2014). Instead, we speculate that anticipatory signals from higher order skeletomotor regions are relayed to the SC (Distler and Hoffmann 2015; Fries 1984, 1985), providing a means to preset SC activity before the arrival of visually related information so that the resulting SLR reflects both stimulus location relative to the hand and the preselected motor plan.

ACKNOWLEDGMENTS

We thank D. Park for assistance in data collection for *experiment 1* and H. Ohashi for programming assistance with the modified updated maximum likelihood procedure for *experiment 3*.

GRANTS

This work was supported by Natural Sciences and Engineering Research Council of Canada (NSERC) Grants RGPIN-311680 (to B. D. Corneil), RGPIN-238338 (to P. L. Gribble), and RGPIN-2015-06714 (to J. A. Pruszynski), Canadian Institutes of Health Research Grant MOP-93796 (to B. D. Corneil), and an NSERC Alexander Graham Bell Canada Graduate Doctoral Scholarship (to C. Gu). J. A. Pruszynski received a salary award from the Canada Research Chairs program.

DISCLOSURES

No conflicts of interest, financial or otherwise, are declared by the authors.

AUTHOR CONTRIBUTIONS

C.G., J.A.P., P.L.G., and B.D.C. conceived and designed research; C.G. performed experiments; C.G. analyzed data; C.G., J.A.P., P.L.G., and B.D.C. interpreted results of experiments; C.G. prepared figures; C.G. and B.D.C. drafted manuscript; C.G., J.A.P., P.L.G., and B.D.C. edited and revised manuscript; C.G., J.A.P., P.L.G., and B.D.C. approved final version of manuscript.

REFERENCES

- Alstermark B, Isa T. Circuits for skilled reaching and grasping. *Annu Rev Neurosci* 35: 559–578, 2012. doi:10.1146/annurev-neuro-062111-150527.
- Batista AP, Buneo CA, Snyder LH, Andersen RA. Reach plans in eye-centered coordinates. *Science* 285: 257–260, 1999. doi:10.1126/science.285.5425.257.
- Buneo CA, Jarvis MR, Batista AP, Andersen RA. Direct visuomotor transformations for reaching. *Nature* 416: 632–636, 2002. doi:10.1038/416632a.
- Carlton LG. Processing visual feedback information for movement control. *J Exp Psychol Hum Percept Perform* 7: 1019–1030, 1981. doi:10.1037/0096-1523.7.5.1019.
- Cashaback JGA, Cluff T, Potvin JR. Muscle fatigue and contraction intensity modulates the complexity of surface electromyography. *J Electromyogr Kinesiol* 23: 78–83, 2013. doi:10.1016/j.jelekin.2012.08.004.

- Chapman BB, Corneil BD.** Neuromuscular recruitment related to stimulus presentation and task instruction during the anti-saccade task. *Eur J Neurosci* 33: 349–360, 2011. doi:10.1111/j.1460-9568.2010.07496.x.
- Cisek P, Kalaska JF.** Neural correlates of reaching decisions in dorsal premotor cortex: specification of multiple direction choices and final selection of action. *Neuron* 45: 801–814, 2005. doi:10.1016/j.neuron.2005.01.027.
- Confais J, Kilavik BE, Ponce-Alvarez A, Riehle A.** On the anticipatory precise activity in motor cortex. *J Neurosci* 32: 15359–15368, 2012. doi:10.1523/JNEUROSCI.1768-12.2012.
- Corneil BD, Munoz DP.** Overt responses during covert orienting. *Neuron* 82: 1230–1243, 2014. doi:10.1016/j.neuron.2014.05.040.
- Corneil BD, Munoz DP, Chapman BB, Admans T, Cushing SL.** Neuro-muscular consequences of reflexive covert orienting. *Nat Neurosci* 11: 13–15, 2008. doi:10.1038/nn2023.
- Corneil BD, Olivier E, Munoz DP.** Visual responses on neck muscles reveal selective gating that prevents express saccades. *Neuron* 42: 831–841, 2004. doi:10.1016/S0896-6273(04)00267-3.
- Crawford JD, Medendorp WP, Marotta JJ.** Spatial transformations for eye-hand coordination. *J Neurophysiol* 92: 10–19, 2004. doi:10.1152/jn.00117.2004.
- Day BL, Brown P.** Evidence for subcortical involvement in the visual control of human reaching. *Brain* 124: 1832–1840, 2001. doi:10.1093/brain/124.9.1832.
- Day BL, Lyon IN.** Voluntary modification of automatic arm movements evoked by motion of a visual target. *Exp Brain Res* 130: 159–168, 2000. doi:10.1007/s002219900218.
- Desmurget M, Epstein CM, Turner RS, Prablanc C, Alexander GE, Grafton ST.** Role of the posterior parietal cortex in updating reaching movements to a visual target. *Nat Neurosci* 2: 563–567, 1999. doi:10.1038/9219.
- Diedrichsen J, Nambisan R, Kennerley SW, Ivry RB.** Independent on-line control of the two hands during bimanual reaching. *Eur J Neurosci* 19: 1643–1652, 2004. doi:10.1111/j.1460-9568.2004.03242.x.
- Distler C, Hoffmann K-P.** Direct projections from the dorsal premotor cortex to the superior colliculus in the macaque (*Macaca mulatta*). *J Comp Neurol* 523: 2390–2408, 2015. doi:10.1002/cne.23794.
- Donders FC.** On the speed of mental processes. *Acta Psychol (Amst)* 30: 412–431, 1969. doi:10.1016/0001-6918(69)90065-1.
- Fautrelle L, Prablanc C, Berret B, Ballay Y, Bonnetblanc F.** Pointing to double-step visual stimuli from a standing position: very short latency (express) corrections are observed in upper and lower limbs and may not require cortical involvement. *Neuroscience* 169: 697–705, 2010. doi:10.1016/j.neuroscience.2010.05.014.
- Franklin DW, Reichenbach A, Franklin S, Diedrichsen J.** Temporal evolution of spatial computations for visuomotor control. *J Neurosci* 36: 2329–2341, 2016. doi:10.1523/JNEUROSCI.0052-15.2016.
- Fries W.** Cortical projections to the superior colliculus in the macaque monkey: a retrograde study using horseradish peroxidase. *J Comp Neurol* 230: 55–76, 1984. doi:10.1002/cne.902300106.
- Fries W.** Inputs from motor and premotor cortex to the superior colliculus of the macaque monkey. *Behav Brain Res* 18: 95–105, 1985. doi:10.1016/0166-4328(85)90066-X.
- Gandhi NJ, Katnani HA.** Motor functions of the superior colliculus. *Annu Rev Neurosci* 34: 205–231, 2011. doi:10.1146/annurev-neuro-061010-113728.
- Gaveau V, Pisella L, Priot AE, Fukui T, Rossetti Y, Pélisson D, Prablanc C.** Automatic online control of motor adjustments in reaching and grasping. *Neuropsychologia* 55: 25–40, 2014. doi:10.1016/j.neuropsychologia.2013.12.005.
- Goonetilleke SC, Katz L, Wood DK, Gu C, Huk AC, Corneil BD.** Cross-species comparison of anticipatory and stimulus-driven neck muscle activity well before saccadic gaze shifts in humans and nonhuman primates. *J Neurophysiol* 114: 902–913, 2015. doi:10.1152/jn.00230.2015.
- Gu C, Wood DK, Gribble PL, Corneil BD.** A trial-by-trial window into sensorimotor transformations in the human motor periphery. *J Neurosci* 36: 8273–8282, 2016. doi:10.1523/JNEUROSCI.0899-16.2016.
- Himmelbach M, Linzenbold W, Ilg UJ.** Dissociation of reach-related and visual signals in the human superior colliculus. *Neuroimage* 82: 61–67, 2013. doi:10.1016/j.neuroimage.2013.05.101.
- Klaes C, Westendorff S, Chakrabarti S, Gail A.** Choosing goals, not rules: deciding among rule-based action plans. *Neuron* 70: 536–548, 2011. doi:10.1016/j.neuron.2011.02.053.
- Kwan HC, MacKay WA, Murphy JT, Wong YC.** Distribution of responses to visual cues for movement in precentral cortex or awake primates. *Neurosci Lett* 24: 123–128, 1981. doi:10.1016/0304-3940(81)90234-2.
- Linzenbold W, Himmelbach M.** Signals from the deep: reach-related activity in the human superior colliculus. *J Neurosci* 32: 13881–13888, 2012. doi:10.1523/JNEUROSCI.0619-12.2012.
- Luce RD.** *Response Times: Their Role in Inferring Elementary Mental Organization*. New York: Oxford University Press, 1986.
- Lünenburger L, Kleiser R, Stuphorn V, Miller LE, Hoffmann KP.** A possible role of the superior colliculus in eye-hand coordination. *Prog Brain Res* 134: 109–125, 2001. doi:10.1016/S0079-6123(01)34009-8.
- MacKay WA, Crammond DJ.** Neuronal correlates in posterior parietal lobe of the expectation of events. *Behav Brain Res* 24: 167–179, 1987. doi:10.1016/0166-4328(87)90055-6.
- Mauritz KH, Wise SP.** Premotor cortex of the rhesus monkey: neuronal activity in anticipation of predictable environmental events. *Exp Brain Res* 61: 229–244, 1986. doi:10.1007/BF00239513.
- Medendorp WP, Goltz HC, Vilis T, Crawford JD.** Gaze-centered updating of visual space in human parietal cortex. *J Neurosci* 23: 6209–6214, 2003.
- Norman RW, Komi PV.** Electromechanical delay in skeletal muscle under normal movement conditions. *Acta Physiol Scand* 106: 241–248, 1979. doi:10.1111/j.1748-1716.1979.tb06394.x.
- Oostwoud Wijdenes L, Brenner E, Smeets JBJ.** Fast and fine-tuned corrections when the target of a hand movement is displaced. *Exp Brain Res* 214: 453–462, 2011. doi:10.1007/s00221-011-2843-4.
- Pesaran B, Nelson MJ, Andersen RA.** Dorsal premotor neurons encode the relative position of the hand, eye, and goal during reach planning. *Neuron* 51: 125–134, 2006. doi:10.1016/j.neuron.2006.05.025.
- Philipp R, Hoffmann KP.** Arm movements induced by electrical microstimulation in the superior colliculus of the macaque monkey. *J Neurosci* 34: 3350–3363, 2014. doi:10.1523/JNEUROSCI.0443-13.2014.
- Pisella L, Gréa H, Tilikete C, Vighetto A, Desmurget M, Rode G, Boisson D, Rossetti Y.** An ‘automatic pilot’ for the hand in human posterior parietal cortex: toward reinterpreting optic ataxia. *Nat Neurosci* 3: 729–736, 2000. doi:10.1038/76694.
- Pruszynski JA, Johansson RS, Flanagan JR.** A rapid tactile-motor reflex automatically guides reaching toward handheld objects. *Curr Biol* 26: 788–792, 2016. doi:10.1016/j.cub.2016.01.027.
- Pruszynski JA, King GL, Boisse L, Scott SH, Flanagan JR, Munoz DP.** Stimulus-locked responses on human arm muscles reveal a rapid neural pathway linking visual input to arm motor output. *Eur J Neurosci* 32: 1049–1057, 2010. doi:10.1111/j.1460-9568.2010.07380.x.
- Reynolds RF, Day BL.** Direct visuomotor mapping for fast visually-evoked arm movements. *Neuropsychologia* 50: 3169–3173, 2012. doi:10.1016/j.neuropsychologia.2012.10.006.
- Rezvani S, Corneil BD.** Recruitment of a head-turning synergy by low-frequency activity in the primate superior colliculus. *J Neurophysiol* 100: 397–411, 2008. doi:10.1152/jn.90223.2008.
- Rodgers CK, Munoz DP, Scott SH, Paré M.** Discharge properties of monkey tectoreticular neurons. *J Neurophysiol* 95: 3502–3511, 2006. doi:10.1152/jn.00908.2005.
- Schiller PH, Malpeli JG, Schein SJ.** Composition of geniculostriate input to superior colliculus of the rhesus monkey. *J Neurophysiol* 42: 1124–1133, 1979. doi:10.1152/jn.1979.42.4.1124.
- Shen Y, Richards VM.** A maximum-likelihood procedure for estimating psychometric functions: thresholds, slopes, and lapses of attention. *J Acoust Soc Am* 132: 957–967, 2012. doi:10.1121/1.4733540.
- Snyder LH, Batista AP, Andersen RA.** Change in motor plan, without a change in the spatial locus of attention, modulates activity in posterior parietal cortex. *J Neurophysiol* 79: 2814–2819, 1998. doi:10.1152/jn.1998.79.5.2814.
- Snyder LH, Dickinson AR, Calton JL.** Preparatory delay activity in the monkey parietal reach region predicts reach reaction times. *J Neurosci* 26: 10091–10099, 2006. doi:10.1523/JNEUROSCI.0513-06.2006.
- Soechting JF, Lacquaniti F.** Modification of trajectory of a pointing movement in response to a change in target location. *J Neurophysiol* 49: 548–564, 1983. doi:10.1152/jn.1983.49.2.548.
- Song JH, McPeck RM.** Neural correlates of target selection for reaching movements in superior colliculus. *J Neurophysiol* 113: 1414–1422, 2015. doi:10.1152/jn.00417.2014.
- Song JH, Rafal RD, McPeck RM.** Deficits in reach target selection during inactivation of the midbrain superior colliculus. *Proc Natl Acad Sci USA* 108: E1433–E1440, 2011. doi:10.1073/pnas.1109656108.
- Stavisky SD, Kao JC, Ryu SI, Shenoy KV.** Motor cortical visuomotor feedback activity is initially isolated from downstream targets in output-null neural state space dimensions. *Neuron* 95: 195.e9–208.e9, 2017. doi:10.1016/j.neuron.2017.05.023.

- Stewart BM, Gallivan JP, Baugh LA, Flanagan JR.** Motor, not visual, encoding of potential reach targets. *Curr Biol* 24: R953–R954, 2014. doi:10.1016/j.cub.2014.08.046.
- Stuphorn V, Bauswein E, Hoffmann KP.** Neurons in the primate superior colliculus coding for arm movements in gaze-related coordinates. *J Neurophysiol* 83: 1283–1299, 2000. doi:10.1152/jn.2000.83.3.1283.
- Stuphorn V, Hoffmann KP, Miller LE.** Correlation of primate superior colliculus and reticular formation discharge with proximal limb muscle activity. *J Neurophysiol* 81: 1978–1982, 1999. doi:10.1152/jn.1999.81.4.1978.
- Tanji J, Evarts EV.** Anticipatory activity of motor cortex neurons in relation to direction of an intended movement. *J Neurophysiol* 39: 1062–1068, 1976. doi:10.1152/jn.1976.39.5.1062.
- Weinrich M, Wise SP.** The premotor cortex of the monkey. *J Neurosci* 2: 1329–1345, 1982.
- Welford AT.** Choice reaction time: basis concepts. In: *Reaction Times*, edited by Welford AT. New York: Academic, 1980, p. 73–128.
- Werner W, Dannenberg S, Hoffmann KP.** Arm-movement-related neurons in the primate superior colliculus and underlying reticular formation: comparison of neuronal activity with EMGs of muscles of the shoulder, arm and trunk during reaching. *Exp Brain Res* 115: 191–205, 1997. doi:10.1007/PL00005690.
- Wong AL, Goldsmith J, Krakauer JW.** A motor planning stage represents the shape of upcoming movement trajectories. *J Neurophysiol* 116: 296–305, 2016. doi:10.1152/jn.01064.2015.
- Wood DK, Gu C, Corneil BD, Gribble PL, Goodale MA.** Transient visual responses reset the phase of low-frequency oscillations in the skeletomotor periphery. *Eur J Neurosci* 42: 1919–1932, 2015. doi:10.1111/ejn.12976.
- Wurtz RH, Goldberg ME.** Activity of superior colliculus in behaving monkey. 3. Cells discharging before eye movements. *J Neurophysiol* 35: 575–586, 1972. doi:10.1152/jn.1972.35.4.575.

